PHYSICAL REVIEW B VOLUME 1, NUMBER 12 15 JUNE 1970

Anharmonic Interaction in Aluminum. I

T. R. Koehler

IBM Research Laboratory, San Jose, California 95114

and

N. S. Gillis and Duane C. Wallace

*Sandia Laboratories, Albuquerque, New Mexico** 87115

(Received 3 November 1969)

Anharmonic linewidths and frequency shifts have been calculated as a function of temperature for Al, employing an effective interionic interaction derived from a model pseudopotential. Calculations have been carried out along principal symmetry directions at 80 and 300 K and comparison is made with the experimental data of Stedman and Nilsson and with the recent calculations of Högberg and Sandström. The structure of the one-phonon spectral function at 300 K for selected longitudinal phonons is examined in detail and discussed. The presence of a significant asymmetry in the one-phonon peak for the (0.8, 0, 0) longitudinal mode is pointed out.

I. INTRODUCTION

It is certainly one of the more gratifying aspects of the pseudopotential theory of metals that the low-temperature lattice vibrational spectra of the simple metals can be adequately described within the context of this theory and in the harmonic approximation.[1-8] In addition, the theory has been successful in describing first-order anharmonic properties, such as the thermal-expansion coefficient[7] and the third-order elastic constants.[9] Until the recent calculations of Högberg and Sandström (HS)[10] on Al and Buyers and Cowley[11] on K, however, none of the model potential approaches had been applied to the calculation of second-order anharmonic properties in the simple metals, although it is clear that such calculations would provide a further test of the validity of these models. It is intuitively appealing to attempt to adopt in its entirety the effective two-body interaction potential which has its genesis in the neutral pseudoatom concept[12] of the metal, to proceed to calculate third- and fourth-order derivatives of this potential, and hence to employ standard anharmonic perturbation theory to calculate those properties which are of interest. This, in principle, would be a well-defined straightforward procedure were it not for one difficulty. As is well known, in calculating the effective ion-electron-ion contribution to the energy of the crystal, one can proceed with an expansion in powers of the atomic displacements with a subsequent utilization of perturbation theory to the appropriate order in these displacements.[2] It is immediately clear, then, that a rigorous treatment of anharmonic effects should include terms of third and higher order in the electron-phonon interaction, whereas the effective interionic potential derived from the neutral pseudoatom picture is correct only to second order in this interaction. This point has been discussed in detail by Buyers and Cowley,[11] who emphasize the difficulty of including these additional terms in any quantitative anharmonic calculations.

There is an alternative approach, however, which allows one to circumvent this difficulty. If the perturbation is taken to be the pseudopotential, rather than the atomic displacements, then the total energy of the conduction electrons may be calculated to second order in the pseudopotential for arbitrary positions of the atoms.[1] Then the effective interionic potential is correct to all orders in the atomic displacements, but is correct only to second order in the pseudopotential. The second-, third-, and higher-order derivatives of this potential are all given correctly to leading order in the pseudopotential, namely, to second order, and hence the harmonic and anharmonic properties can be calculated correctly to leading order in the pseudopotential. This has been the approach in previous calculations, and it has been shown that the phonon frequencies are the same as those obtained from the neutral pseudoatom picture.[7]

We begin the discussion in Sec. II with a description of the model potential employed in the present calculation on Al. We then proceed immediately to the calculation of frequency shifts and lifetimes for phonons along the [100], [110], and [111] symmetry directions at 80 and

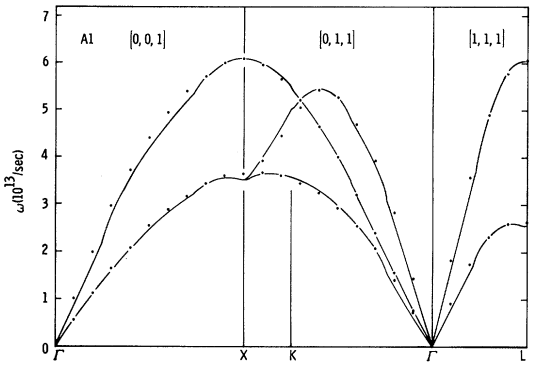

FIG. 1. Model potential fit to the phonon dispersion curves of Al at 80 K. Experimental points from the data of Stedman *et al.* (Ref. 14) are represented by solid circles.

300 K. The changes in the lifetimes and frequencies of these phonons with temperature are compared with the experimental results of Stedman and Nilsson[13]; reasonably good agreement with experiment is found. Comparison of the present calculated values with the recent calculations of HS[10] reveals significant differences and these are discussed. The final portion of the paper is devoted to a detailed examination of the structure of the one-phonon spectral function at 300 K for selected phonons in regions of large attenuation.

II. MODEL POTENTIAL

In a previous paper,[8] the parameters of a Harrison modified point-ion potential[1] were determined to obtain the best over-all fit to the measured dispersion curves[14] for Al at 80 K. The phonon frequencies and eigenvectors were determined to within an estimated numerical accuracy of 0.5% and the average magnitude of deviation of the calculated curves from the experimental points was 3%. For ease of reference, the calculated dispersion curves are reproduced in Fig. 1.

For the Harrison modified point-ion model the bare-pseudopotential form factor may be written

$$V_b(q) = (1/\Omega_a)[-4\pi z e^2/q^2 + \beta/(1+q^2\rho^2)^2] \quad , \tag{1}$$

where Ω_a is the volume per atom; β and ρ are parameters relating to the ion core. The screened form factor takes the form

$$V_s(q) = V_b(q)/[1+(\epsilon_q - 1)(1-g_q)] \quad ,$$
$$g_q = q^2/[2(q^2 + \xi k_F^2)] \quad , \tag{2}$$

where ϵ_q is the Hartree dielectric function and $(1-g_q)$ is the Hubbard-Sham exchange and correlation correction factor. ξ is a parameter to be determined from the electron-gas compressibility, and k_F is the magnitude of the Fermi wave vector. For the fit shown in Fig. 1, the parameters entering into the bare-ion form factor have the values

$$\beta = 47.5 \text{ Ry } a_0^3, \quad \rho = 0.24\ a_0 \quad .$$

The effective interionic interaction consists of the direct Coulomb interaction between ion cores plus the indirect ion-electron-ion interaction derived from $V_b(q)$ and the Hartree dielectric function. This effective interaction between ions has the form[1]

$$V(r) = \frac{z^2e^2}{r} + \frac{2z^2e^2}{\pi}\int_0^\infty F(q)\,\frac{\sin qr}{qr}\,dq \quad ,$$
$$F(q) = -\left(\frac{\Omega_a q^2}{4\pi z e^2}\,V_b(q)\right)^2\left(\frac{\epsilon_q - 1}{1+(\epsilon_q-1)(1-g_q)}\right) \quad . \tag{3}$$

$V(r)$ and its first four derivatives were determined from (3) with a numerical accuracy of ~0.1%. Table I tabulates the values of $V(r)$ and $(d/rdr)^n V(r)$ $(n = 1, 2, \ldots, 4)$ for 12 shells of neighbors in Al. In addition, $V(r)$ is plotted as a function of the ion separation in Fig. 2. It can be shown that the direct Coulomb part of $V(r)$ is cancelled for distances greater than about half the nearest-neigh-

TABLE I. Calculated values of $V_n \equiv (d/rdr)^n V(r)$ (Ry/a_0^{2n}) for 12 shells of neighbors. The nearest-neighbor distance is that appropriate to 80 K.

Shell	Distance (a_0)	V_0	V_1	V_2	V_3	V_4
1	5.38950	2.026×10^{-4}	-9.764×10^{-4}	9.826×10^{-4}	-6.737×10^{-4}	3.456×10^{-4}
2	7.62190	-2.086×10^{-3}	-3.953×10^{-5}	5.916×10^{-5}	-1.565×10^{-6}	-3.464×10^{-6}
3	9.33489	1.510×10^{-4}	1.106×10^{-4}	-2.521×10^{-5}	-2.841×10^{-7}	8.907×10^{-7}
4	10.77900	-7.046×10^{-5}	-5.750×10^{-5}	4.815×10^{-6}	1.412×10^{-6}	-2.989×10^{-7}
5	12.05129	-1.696×10^{-4}	3.407×10^{-5}	2.047×10^{-6}	-9.090×10^{-7}	2.311×10^{-8}
6	13.20152	1.870×10^{-4}	1.139×10^{-6}	-3.694×10^{-6}	1.839×10^{-7}	5.891×10^{-8}
7	14.25928	-2.852×10^{-5}	-1.806×10^{-5}	1.147×10^{-6}	2.499×10^{-7}	-3.289×10^{-8}
8	15.24381	-1.079×10^{-4}	7.615×10^{-6}	1.343×10^{-6}	-1.639×10^{-7}	-1.133×10^{-8}
9	16.16850	5.251×10^{-5}	8.970×10^{-6}	-9.322×10^{-7}	-8.185×10^{-8}	1.538×10^{-8}
10	17.04310	6.884×10^{-5}	-5.697×10^{-6}	-6.608×10^{-7}	8.952×10^{-8}	4.474×10^{-9}
11	17.87495	-3.810×10^{-5}	-5.744×10^{-6}	5.412×10^{-7}	4.706×10^{-8}	-7.429×10^{-9}
12	18.66978	-5.620×10^{-5}	3.358×10^{-6}	4.837×10^{-7}	-4.430×10^{-8}	-3.199×10^{-9}

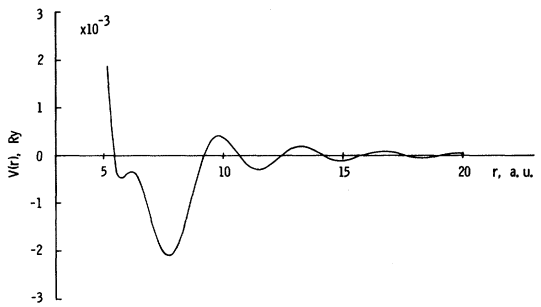

FIG. 2. The effective interionic potential for Al plotted as a function of ion separation.

bor separation, so that $V(r)$ is entirely of a screened nature with the asymptotic behavior $r^{-3}\cos k_F r$.[1] The values of the spatial derivatives of $V(r)$ for eight shells of neighbors in coordinate space were incorporated into the anharmonic calculation of widths and frequency shifts. At this point, it should be noted that the present calculation deals directly with the effective $V(r)$ and its spatial derivatives in coordinate space, whereas the calculation of HS employs the Fourier transform of $V(r)$ in reciprocal space. By performing lattice sums in coordinate space, we treat the small $\vec{r}$ – hence, large $\vec{q}$ – components of V and its spatial derivatives most accurately. These large $\vec{q}$ components are in fact quite important in the calculation of the anharmonic shifts and widths. We will return to this point in detail in Sec. IV.

III. ANHARMONIC LINEWIDTHS AND FREQUENCY SHIFTS

It is well known that the observed cross section for the scattering of neutrons by a crystal may be decomposed into a rapidly varying part – the so-called one-phonon part – and a part which is slowly varying and gives rise to the multiphonon background.[15] The rapidly varying part, which resonates at the one-phonon frequencies, may be further decomposed into two contributions – a "pure" one-phonon part plus a part representing the interference of the one-phonon and multiphonon processes. In the approximation in which one neglects interference effects,[16] the one-phonon contribution to the scattering cross section is given in terms of the one-phonon Green's function $G_{\lambda\lambda'}(\vec{q}, \Omega)$ as[15]

$$\begin{aligned}\mathrm{Im}\, G_{\lambda\lambda}(\vec{q}, \Omega + i0^+)/[e^{\beta\Omega} - 1] &= [e^{\beta\Omega} - 1]^{-1} \\ &\times \mathrm{Im}(2\omega_\lambda(\vec{q})/\{[\omega_\lambda(\vec{q})]^2 - \Omega^2 \\ &+ 2\omega_\lambda(\vec{q})\Delta_{\lambda\lambda}(\vec{q}, \Omega) - 2i\omega_\lambda(\vec{q})\Gamma_{\lambda\lambda}(\vec{q}, \Omega)\}) \quad . \qquad (4)\end{aligned}$$

$\omega_\lambda(\vec{q})$ is the bare-phonon frequency in the absence of anharmonicity and Δ, Γ are the real and imaginary parts of the phonon self-energy, respectively. For fixed $\vec{q}$, λ, the position of the peak in (4) defines the renormalized phonon frequency ω_R. If Δ, Γ are assumed small, we have the approximate relation

$$\omega_R(\vec{q}, \lambda) \approx \omega_\lambda(\vec{q}) + \Delta_{\lambda\lambda}(q, \omega_\lambda(\vec{q})) \quad , \qquad (5a)$$

with the full width at half-maximum given approximately by

$$W(\vec{q}, \lambda) \approx 2\Gamma_{\lambda\lambda}(q, \omega_\lambda(q)) \, . \qquad (5b)$$

The exact method of determining the renormalized phonon frequency may be quite important, especially if the system is so highly anharmonic that the approximations (5a)–(5b) are poor.[17] In this case, ω_R must be identified with the position of the true maximum in $\mathrm{Im}\, G(\Omega)$.

The expressions for Δ and Γ including cubic and quartic anharmonic contributions are by now well enough known so as not to necessitate reproducing them here.[18] The quasiharmonic frequency shift, arising from the thermal expansion of the crystal, was included by performing the calculations at the observed lattice constant. As the basis of the anharmonic calculation we employed the phonon frequencies and eigenvectors of Ref. 8, calculated on a bcc mesh in q space consisting of 8000 points in the first Brillouin zone. All calculations were carried out on an IBM 360/91 computer. The greatest uncertainty in the calculations arises from the approximations $P/x \approx x/(x^2 + \epsilon^2)$ and $\pi\delta(x) \approx \epsilon/(x^2 + \epsilon^2)$, where ϵ is small but finite. For each q point for which the anharmonic calculation was carried out, plots of $\Gamma(\Omega)$, $\Delta(\Omega)$, and $\mathrm{Im}\, G(\Omega)$ were made as a function of Ω. The criterion used in choosing the grid size in q space and the magnitude of ϵ was the over-all stability of the plots of $\Delta(q, \Omega)$, $\Gamma(q, \Omega)$ as functions of both q and Ω when changes were made in the mesh size and in the magnitude of ϵ. After considerable experimentation a value of 0.10×10^{13} rad/sec was chosen for ϵ. It is believed that the calculations represent a numerical accuracy of about 5%.

Before closing this section, it should be pointed out that there is, in addition to the anharmonic contribution to the phonon damping, a contribution arising from the electron-phonon interaction.[19,20] Although this contribution may be important at low temperatures in determining the magnitude of the phonon linewidth, its contribution to the temperature dependence is negligible. In what follows we are primarily interested in the change with temperature of the phonon linewidths. Hence, we are justified in neglecting this contribution to the phonon damping.

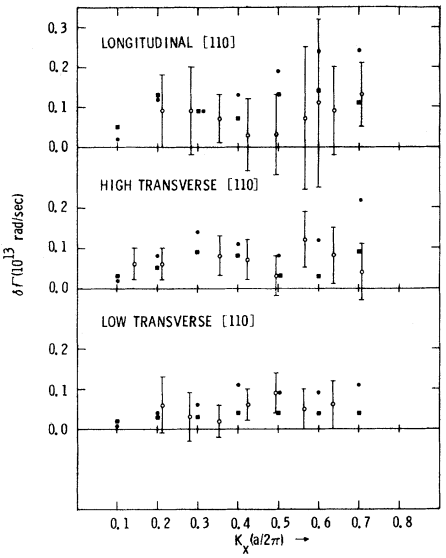

FIG. 3. Increase in phonon linewidth with temperature $[\delta\Gamma \equiv \Gamma(300\ \mathrm{K}) - \Gamma(80\ \mathrm{K})]$ for the symmetry direction [110]. The experimental points are given by open circles and the calculated points of the present work are denoted by solid squares. The calculated values of Högberg and Sandström (Ref. 10) are shown by solid circles.

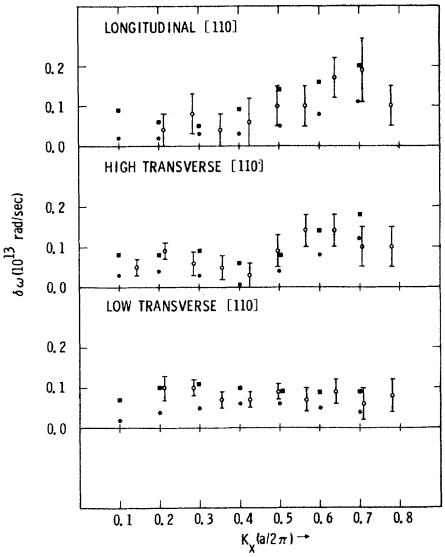

FIG. 5. Decrease in phonon frequencies with temperature $[\delta\omega \equiv \omega(80\ \mathrm{K}) - \omega(300\ \mathrm{K})]$ for the symmetry direction [110]. Experimental and calculated points are denoted as in Fig. 3.

IV. RESULTS

The real and imaginary parts of the phonon self-energy $\Delta_\lambda(\vec{q}, \Omega)$, $\Gamma_\lambda(\vec{q}, \Omega)$ were evaluated at the two temperatures 80 and 300 K for fixed $\vec{q}$ and as a function of Ω. Calculations were carried out along the symmetry directions [100] and [110] at wave-number intervals $\Delta q_x(a/2\pi) = 0.1$ and along the symmetry direction [111] for $\Delta q_x(a/2\pi) = 0.05$. Full plots were made of $\Gamma(\Omega)$, $\Delta(\Omega)$, and Im $G(\Omega)$ as functions of Ω at each $\vec{q}$ point. Thus, it was possible to ascertain the magnitude of the difference between the approximate ω_R, W defined in (5a) and (5b) and the ω_R, W obtained by locating the true maximum of Im G. With only one exception, which will be discussed below, the approximations (5a) and (5b) sufficed for the present calculations. Thus, the calculated values plotted in Figs. 3–6 and quoted in Table II are those appropriate to these approximations.

The increase in the phonon half-width with temperature, $\delta\Gamma \equiv \Gamma(300\ \mathrm{K}) - \Gamma(80\ \mathrm{K})$, and the decrease with temperature of the phonon frequencies, $\delta\omega \equiv \omega_R(80\ \mathrm{K}) - \omega_R(300\ \mathrm{K})$, are plotted in Figs. 3 and 4 and 5 and 6, respectively, together with the experimental data of Stedman and Nilsson.[13] The over-all agreement of the present calculations with experiment is quite satisfactory, although it is clear that the large experimental errors preclude making any definitive statements. Also plotted in

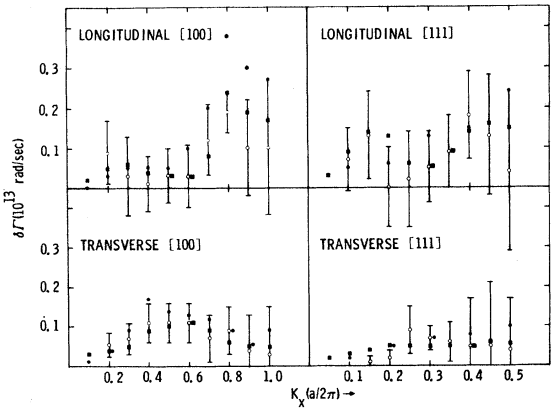

FIG. 4. Same as Fig. 3 but for the symmetry directions [100] and [111].

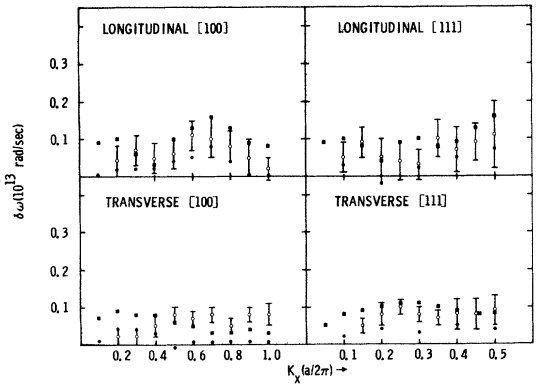

FIG. 6. Same as Fig. 5 but for the symmetry directions [100] and [111].

TABLE II. Calculated and experimental (Ref. 13) values for the changes with temperature of phonon widths and shifts in Al.

Wave vector	Mode	$\Gamma(300\ \mathrm{K}) - \Gamma(80\ \mathrm{K})$ (10^{13} rad/sec) Calc	Expt	$\omega(300\ \mathrm{K}) - \omega(80\ \mathrm{K})$ (10^{13} rad/sec) Calc	Expt
(0.1, 0.0, 0.0)	L	0.020		−0.086	
	T	0.026		−0.074	
(0.2, 0.0, 0.0)	L	0.051	0.90±0.08	−0.099	−0.04±0.04
	T	0.043	0.06±0.03	−0.087	−0.02±0.02
(0.3, 0.0, 0.0)	L	0.057	0.03±0.10	−0.062	−0.07±0.04
	T	0.053	0.07±0.04	−0.082	−0.02±0.02
(0.4, 0.0, 0.0)	L	0.040	0.01±0.07	−0.031	−0.05±0.04
	T	0.093	0.11±0.05	−0.081	−0.05±0.03
(0.5, 0.0, 0.0)	L	0.028	0.03±0.07	−0.096	−0.06±0.04
	T	0.104	0.11±0.05	−0.057	−0.08±0.02
(0.6, 0.0, 0.0)	L	0.035	0.03±0.08	−0.134	−0.11±0.04
	T	0.107	0.11±0.05	−0.047	−0.07±0.02
(0.7, 0.0, 0.0)	L	0.083	0.12±0.09	−0.155	−0.10±0.05
	T	0.090	0.07±0.06	−0.034	−0.08±0.02
(0.8, 0.0, 0.0)	L	0.239	0.12±0.05	−0.131	−0.08±0.06
	T	0.061	0.09±0.06	−0.033	−0.05±0.02
(0.9, 0.0, 0.0)	L	0.191	0.10±0.12	−0.091	−0.05±0.05
	T	0.048	0.04±0.09	−0.037	−0.08±0.02
(1.0, 0.0, 0.0)	L	0.166	0.10±0.17	−0.083	−0.02±0.03
	T	0.052	0.03±0.12	−0.025	−0.08±0.03
(0.05, 0.05, 0.05)	L	0.033		−0.086	
	T	0.016		−0.054	
(0.10, 0.10, 0.10)	L	0.087	0.07±0.08	−0.099	−0.05±0.04
	T	0.031		−0.080	
(0.15, 0.15, 0.15)	L	0.139	0.13±0.11	−0.077	−0.09±0.04
	T	0.041	0.01±0.01	−0.095	−0.05±0.02
(0.20, 0.20, 0.20)	L	0.135	0.0±0.10	−0.035	−0.05±0.05
	T	0.046	0.02±0.02	−0.103	−0.08±0.03
(0.25, 0.25, 0.25)	L	0.064	0.02±0.12	−0.089	−0.04±0.05
	T	0.049	0.09±0.06	−0.107	−0.10±0.02
(0.30, 0.30, 0.30)	L	0.048	0.05±0.09	−0.097	−0.03±0.04
	T	0.054	0.07±0.03	−0.111	−0.08±0.02
(0.35, 0.35, 0.35)	L	0.092	0.09±0.09	−0.076	−0.10±0.05
	T	0.054	0.06±0.05	−0.101	−0.07±0.02
(0.40, 0.40, 0.40)	L	0.137	0.18±0.11	−0.093	−0.07±0.06
	T	0.053	0.05±0.12	−0.089	−0.08±0.04
(0.45, 0.45, 0.45)	L	0.162	0.13±0.15	−0.133	−0.09±0.05
	T	0.056	0.05±0.16	−0.080	−0.08±0.04
(0.50, 0.50, 0.50)	L	0.149	0.04±0.20	−0.160	−0.11±0.09
	T	0.059	0.04±0.13	−0.078	−0.09±0.04
(0.10, 0.10, 0.0)	L	0.049	See Fig. 3	−0.094	See Fig. 5
	T_1	0.029		−0.081	
	T_2	0.016		−0.066	
(0.20, 0.20, 0.0)	L	0.135		−0.057	
	T_1	0.051		−0.085	
	T_2	0.029		−0.102	
(0.30, 0.30, 0.0)	L	0.089		−0.048	
	T_1	0.089		−0.094	
	T_2	0.035		−0.108	
(0.40, 0.40, 0.0)	L	0.073		−0.086	
	T_1	0.075		−0.056	
	T_2	0.040		−0.103	
(0.50, 0.50, 0.0)	L	0.131		−0.143	
	T_1	0.030		−0.083	
	T_2	0.038		−0.092	
(0.60, 0.60, 0.0)	L	0.139		−0.157	
	T_1	0.031		−0.137	
	T_2	0.038		−0.091	
(0.70, 0.70, 0.0)	L	0.107		−0.198	
	T_1	0.093		−0.178	
	T_2	0.038		−0.088	

Figs. 3–6 are the calculated values of HS and it is obvious that significant differences exist between their results and the results of the present work. We would now like to discuss this point in some detail.

The claim was made in Sec. II of this work that the large wave-vector components of $V(r)$ and its derivatives are important to the calculation of the anharmonic shifts and widths; and, further, that in order to treat these components most accurately, one should work with $V(r)$ and its derivatives directly in coordinate space. Now it is true that for a cubic monatomic lattice a cancellation of these large wave-vector components occurs for wave vectors large compared to a typical wave vector in the first Brillouin zone. However, because of the slow convergence in reciprocal space, this cancellation only becomes effective for reciprocal-lattice vectors with magnitude much greater than the K_{max} chosen by HS, who terminate their reciprocal-lattice sums after 25 shells, corresponding to $(a/2\pi)K_{max} \sim 8$. One can easily verify that the region of reciprocal space for $(a/2\pi)|\vec{K}| > 8$ contributes the following amounts to the spatial derivatives of $V(r)$ at the first-neighbor separation: 22% to $V'(r)$, 10% to $V''(r)$, 40% to $V'''(r)$, and 59% to $V''''(r)$. Only for the initial phonon wave vector $\vec{q}$ very near the zone center will these contributions to $\Delta(\vec{q})$, $\Gamma(\vec{q})$ from the region of reciprocal space outside a sphere of radius K_{max} be negligible. For $\vec{q}$ well into the zone, the error incurred by neglecting the large wave-vector region in reciprocal space may be considerable. In contrast to this, the present calculation employs lattice sums in coordinate space, terminating said sums after eight shells of neighbors. This means that the greatest error in $\Delta(q)$ and $\Gamma(q)$ is incurred for small $\vec{q}$; more specifically, for $(\alpha/2\pi)|\vec{q}| \lesssim 0.1$, a region of little importance in the present calculation. In summary, then, it is possible that the discrepancies between the calculated values of HS and the calculated values of the present work can be attributed to insufficient convergence in the HS reciprocal-lattice sums. A further source of the discrepancy between the two calculations might be the dependence of the third and fourth derivatives of $V(r)$ on the model potential used to fit the dispersion curves. Certainly, the extent to which the anharmonic calculations are model dependent is a point which deserves attention in the future.

In Figs. 7(a)–7(c), we display plots of Im $G(\Omega)$, $\Delta(\Omega)$, and $\Gamma(\Omega)$ for selected longitudinal [100] phonons at 300 K in a region of large attenuation. These figures trace the growth and disappearance of a prominent asymmetry in the peak of the one-phonon spectral function for the longitudinal mode

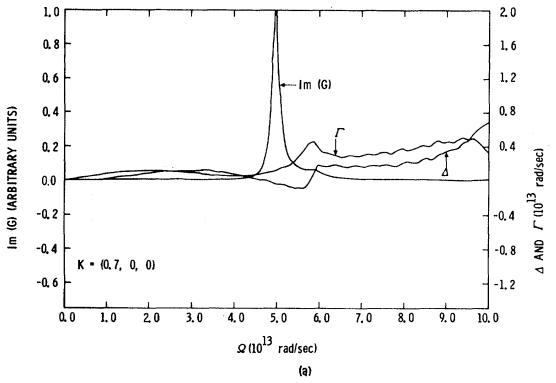

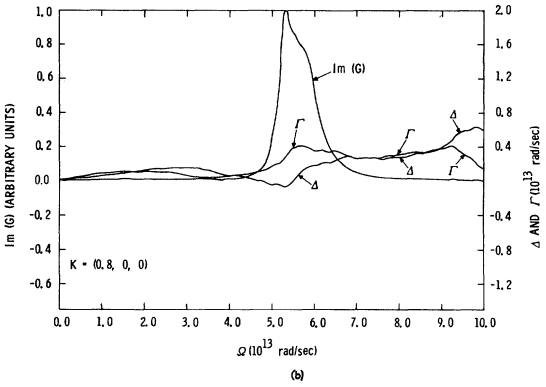

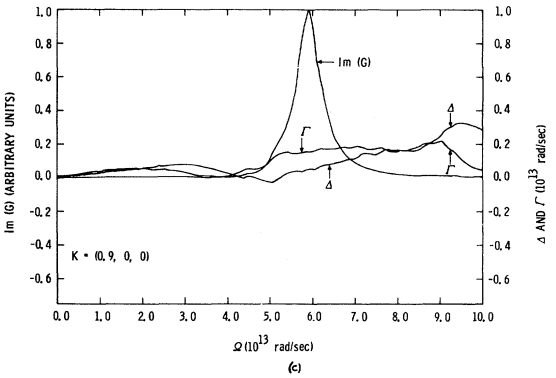

FIG. 7. (a)–(c) One-phonon spectral function Im $(G(\Omega))$ plotted as a function of frequency for selected longitudinal phonons. Also plotted are the real part of the phonon self-energy $\Delta(\Omega)$ and the imaginary part of the self-energy $\Gamma(\Omega)$.

along [100]. This asymmetry, which is not present for $q_x(a/2\pi) = 0.7$, dramatically appears at (0.8, 0, 0), then subsequently disappears as one approaches the zone boundary. For the longitudinal mode (0.8, 0, 0) the difference between the true renormalized phonon frequency and the approximation of Eq. (5a) is about 4%. Although this difference is not particularly significant, the difference between the true half-width and the approximate half-width of Eq. (5b) is more dramatic – 13%. On the other hand, the experimentally derived half-width is probably not representative of the true calculated width, but rather represents a value appropriate to some average of the calculated peak displayed in Fig. 7(b) – assuming the asymmetry is real. The attenuation of the longitudinal mode (0.8, 0, 0) is probably dominated by the decay process in which the longitudinal phonon decays into two transverse phonons with wave vectors near the centers of the hexagonal faces of the Brillouin zone. These hexagonal face centers represent critical points for the low transverse branch of the phonon spectrum and so a high density of final states is expected for the decay process mentioned.[14]

Except for the (0.8, 0, 0) longitudinal mode the one-phonon spectral function associated with all other phonons is to a very good approximation Lorentzian in shape. This has been verified directly by calculating the shape of the spectral function for all of the phonons considered in the present investigation.

V. SUMMARY AND DISCUSSION

In the present work, we have calculated anharmonic linewidths and frequency shifts for Al employing standard anharmonic perturbation theory in conjunction with an effective interionic interaction derived from bare-pseudopotential form factors and a metallic screening function. A Harrison modified point-ion model was employed for the bare-ion core form factors, the parameters of the model being determined by a fit to the phonon dispersion curves at 80 K. There is considerable arbitrariness in the choice of model pseudopotentials. However, a comparison between theory and experiment is not without meaning. Certainly the large experimental errors preclude attaching any particular significance to the agreement between any individual experimental value and theory. However, comparisons of the over-all trend of the measured values with the over-all trend of the theoretical values are significant. On the basis of this criterion we believe that the present calculations show better over-all agreement with experiment than the HS calculation. Furthermore, it is to be noted that the model potential used in the present calculation employs two parameters, whereas the HS calculation employs three.

The considerations outlined in the previous sections lead us to assess the over-all accuracy of the present calculations at 5%, a considerable improvement over the HS quoted accuracy of 25%. It can be argued that the present experimental data do not justify such accuracy. However, since it is particularly difficult to extract the natural width of the phonons from the neutron scattering data, the present investigation should provide a more accurate guide in future experiments for extracting experimental resolution functions. Of particular interest is the fact that except for the (0.8, 0, 0) longitudinal mode – for which a large asymmetry exists – all other phonons exhibit resonance shapes which are Lorentzian in character.

---

*Work supported by the U. S. Atomic Energy Commission.

[1]W. A. Harrison, *Pseudopotentials in the Theory of Metals* (Benjamin, New York, 1966).

[2]L. J. Sham, Proc. Roy. Soc (London) A283, 33 (1965).

[3]S. H. Vosko, R. Taylor, and G. H. Keech, Can. J. Phys. 43, 1187 (1965).

[4]T. Schneider and E. Stoll, Physik Kondensierten Materie 5, 331 (1966); 5, 364 (1966).

[5]A. O. E. Animalu, F. Bonsignori, and V. Bortolani, Nuovo Cimento 44, 159 (1966).

[6]N. W. Ashcroft, J. Phys. C 1, 232 (1968).

[7]D. C. Wallace, Phys. Rev. 176, 832 (1968).

[8]D. C. Wallace, Phys. Rev. 187, 991 (1969).

[9]T. Suzuki, A. V. Granato, and J. F. Thomas, Jr., Phys. Rev. 175, 766 (1968).

[10]T. Högberg and R. Sandström, Phys. Status Solidi 33, 169 (1969).

[11]W. J. L. Buyers and R. A. Cowley, Phys. Rev. 180, 755 (1969).

[12]J. Ziman, Advan. Phys. 13, 89 (1964).

[13]R. Stedman and G. Nilsson, Phys. Rev. 145, 492 (1966).

[14]R. Stedman, L. Almqvist, and G. Nilsson, Phys. Rev. 162, 549 (1967).

[15]V. Ambegaokar, J. Conway, and G. Baym, in *Lattice Dynamics*, edited by R. F. Wallis (Pergamon, New York, 1965), p. 261.

[16]An attempt at assessing the effect of the interference terms on the shape and intensity of the one-phonon scattering cross section was made by A. A. Maradudin and V. Ambegaokar, Phys. Rev. 135, A1071 (1964). They concluded that the interference terms represented only

a small correction to the shape of the one-phonon peak. On the other hand, recent evidence indicates that in certain cases the interference terms may make important contributions to the intensity of the one-phonon scattering. See R. A. Cowley, E. C. Svensson, and W. J. L. Buyers, Phys. Rev. Letters 23, 525 (1969).

[17]T. R. Koehler, Phys. Rev. Letters 22, 777 (1969).
[18]R. A. Cowley, Rept. Progr. Phys. 31, 123 (1968), and references cited therein.
[19]J. J. J. Kokkedee, Physica 28, 893 (1962).
[20]G. Björkman, B. I. Lundqvist, and A. Sjölander, Phys. Rev. 159, 551 (1967).